Plasmonics
https://doi.org/10.1007/s11468-024-02382-6

RESEARCH

Tuneable Terahertz Surface Plasmons Excitation in a Metal-Air-Metal Symmetrical Structure by Relativistic Electron Beam

Pawan Kumar[1] · Neha Verma[2] · Deepak Kumar[1] · Madan Lal[1] · Fateh Singh Gill[1]

Received: 12 April 2024 / Accepted: 6 June 2024

Abstract
One notable issue related to terahertz radiation generation is the tuneability of the source. In this manuscript, we study the properties of plasmons that arise when a beam passes through the gap between the plates. These metallic plates are separated by an air gap. A fast-moving electron beam can propagate in the gap between metallic plates without any divergence due to the minimum value of SPs electric field at the center of structure. As the electron beam is moving through the gap, it resonantly excites the SPs by the Cherenkov interaction between electron beam and SPs, at metal- air interfaces. These THz surface plasmons are transformed into THz radiation. The frequency of generated THz radiation can be tuned with varying the gap between the metallic plates and the electron beam energy. The proposed structure will open the possibility to design a compact source for coherent and tuneable THz radiation generation in broad spectrum regime, which will be useful for medical diagnostics, photonics devices, etc.

Keywords Surface plasmons · Terahertz radiation · Terahertz waveguide · Metallic waveguide

Introduction

Terahertz (THz) radiation frequency lies in the range of 0.1–10 THz and known as THz Gap [1, 2]. THz radiation is novel type radiation and has several unique properties like as quantum and electronic properties of materials, non-ionizing properties, easily penetrates through most polymeric materials and which are often opaque at visible frequencies and also easily absorb in water. Since more than two decades, the Terahertz radiation generation and detection became a fascinating and forefront research area due to large number of diversified applications [2–10]. THz radiation also used as an important tool for studying the benign and malignant brain tumours [11, 12]. Strong field THz radiation is also used to explore the new phenomena including high harmonics generation, and relativistic charged particle acceleration at very high energy (THz-based compact particle accelerators-THz radiation has strong electric field gradient which are beneficial for ultrashort compact and x-ray sources) [13, 14].

Currently, there are many schemes of high-power THz radiation generation with high field, among them high-power laser interaction with solids (metal/semiconductors/dielectrics) and plasmas are widely used [15–17]. Another alternative and important scheme for terahertz radiation generation is based on electron beam. A high energy electron beam moves through a magnetic wiggler/undulator or two different dielectrics materials; it generates the synchrotron/transition THz radiation [18–20]. In current applications, the confined and guided electromagnetic modes are required; these modes are known surface plasma waves (SPWs) or surface plasmons (SPs) [21–23]. These modes are collective oscillations of electrons that propagate at interfaces of conductor or plasma and confined near the interface of different media, their amplitude attenuates in perpendicular direction of propagation. These highly confined modes or SPs have large number of applications including extraordinary transmission, THz plasmonics, plasmonic laser, plasmonic sensors, high harmonics generation, magnetoplasmonics (ultrafast switch), surface-enhanced Raman scattering (SERS), and laser ablation of materials for thin film deposition [24–28].

✉ Pawan Kumar
kumarpawan_30@yahoo.co.in

[1] Department of Physics, Graphic Era (Deemed to be University) University, Dehradun 248002, India

[2] Department of Applied Sciences, Hi-Tech Institute of Engineering and Technology, Ghaziabad, U.P., India

Published online: 15 June 2024

An electron beam or laser beam is widely used for resonant excitation of THz- SPs in various structures including in thin metallic films, graphene, and structured surfaces. The resonant frequency of these SPs can be tuned by the thickness of the film and changing the scale of structured surfaces [29–32]. The alternative approach for electron beam propagation without any divergence is based on conductor-dielectric-conductor or conductor-free space-conductor structure. The SPs have negative refraction at optical frequency in metal-dielectric-metal structure; this structure can control the propagations of surface plasmons, which can manipulate the light at nanoscale [33] and also shows the omnidirectional resonance, at the SPs frequency of the conductor–dielectric interface [34]. A slab-symmetric structure is also used for relativistic electron acceleration and Cherenkov THz radiation generation [35]. The microwave pulse shortening occurs in Cherenkov devices based on slow-wave structures; this is due to the transformation of kinetic energy of relativistic electrons beam into microwave energy [36]. The high-power microwave (HPM) sources based on plasma filled backward oscillators have high efficiency as compared to other backward oscillators, because the plasma in an HPM source is the charge neutralizing effect of positively charged plasma on electron beams [37]. Metallic mesostructured or periodic structures of very thin wires also support the SP modes in infrared or GHz frequency range [38].

In this manuscript, we study the properties of plasmons in THz frequency range that arise when a beam passes through the gap between two metallic plates. The structure supports the field of guided electromagnetic modes or SPs and have minimum value at the middle of the gap, so the electron beam passing through this air gap, experiences a converging force and this electron beam can propagate without any divergence through this gap. These SPs have lower phase velocity than the free space velocity of photon, so SPs can be excited by a moving relativistic electron beam via Cherenkov interaction. A relativistic electron beam moving through this air gap, it resonantly excites the SPs in THz frequency and these THz-SPs are transformed into Coherent THz radiation, when they passing over a periodic structure. In "Mode Structure and Dispersion Relation of Surface Plasmons" section, we derived the modes' structure and dispersion relation; in "Terahertz Surface Plasmons Excitation by a Relativistic Electron Beam" section, the excitation and the growth rate of THz SPs are discussed; and in "Conclusion" section, the result is discussed.

Mode Structure and Dispersion Relation of Surface Plasmons

Consider a symmetrical structure (metal-air-metal) of two parallel metallic (gold) plates, which are separated by finite air gap; this structure supports the surface plasma waves

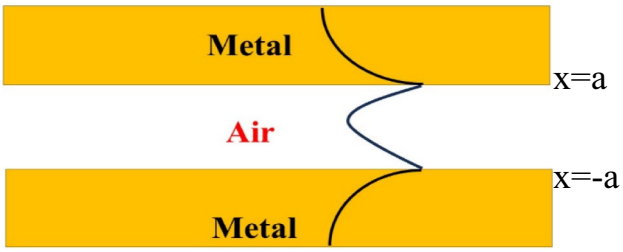

Fig. 1 SPs modes propagation in metal-air-metal symmetrical structure

(SPWs) or surface plasmons (SPs) that are propagating on the metal-air interface, which is shown in Fig. 1. The dispersion relation and modes structure of SPs are obtained by using the following Maxwell's equations,

$$\nabla \times \vec{E} = -\frac{\partial \vec{B}}{\partial t} = +i\omega\mu_0 \vec{H}, \tag{1}$$

$$\nabla \times \vec{H} = \vec{J} + \varepsilon_0 \frac{\partial \vec{E}}{\partial t} = \sigma\vec{E} + \varepsilon_0\left(-i\omega\vec{E}\right) = i\omega\varepsilon'_{eff}\vec{E}, \tag{2}$$

where the total effective permittivity of metal is given by $\varepsilon'_{eff} = \varepsilon_{eff} = \varepsilon_L - \omega_p^2/\omega^2$ for x < -a and x > a, and $\varepsilon'_{eff} = 1$ for -a < x < a. From Eqs. (1) and (2), one may get $\nabla^2\vec{E} - \nabla\left(\nabla.\vec{E}\right) + \frac{\omega^2}{c^2}\varepsilon_{eff}\vec{E} = 0$, and taking the divergence of this equation in media, using the Gauss's law in these two media, i.e., $\varepsilon'_{eff}\nabla.\vec{E} = 0$ i.e. $\nabla.\vec{E} = 0$, this gives equation of surface plasmons

$$\nabla^2\vec{E} + \frac{\omega^2}{c^2}\varepsilon'_{eff}\vec{E} = 0. \tag{3}$$

In terms of x and z components, the wave Eq. (3) can be written as $\frac{\partial^2 E_z}{\partial x^2} + \frac{\partial^2 E_z}{\partial z^2} + \frac{\omega^2}{c^2}\varepsilon'_{eff}\vec{E}_z = 0$, and differential operator is replaced like as $\frac{\partial^2}{\partial z^2} \rightarrow -k_z^2$, one may get

$$\frac{\partial^2 E_z}{\partial x^2} - \alpha^2 E_z = 0, \tag{4}$$

where $\alpha^2 = \alpha_I^2 = k_z^2 - \frac{\omega^2}{c^2}\varepsilon_{eff}$ for x > a and x < -a and $\alpha^2 = \alpha_{II}^2 = k_z^2 - \frac{\omega^2}{c^2}$ for -a < x < a. The modes of different components of mode structure of SPs in different medium can be obtained by solving the Eq. (4) in these different media. In medium x < -a, the solutions of Eq. (4) for z and x components (using $\nabla.\vec{E} = 0$, for x component of electric field) can be written as

$$\begin{aligned} E_z &= A_I \exp(\alpha_I x) exp\left[-i\left(\omega t - k_z z\right)\right], \\ E_x &= -A_I \frac{ik_z}{\alpha_I}\exp(\alpha_I x) exp\left[-i\left(\omega t - k_z z\right)\right]. \end{aligned} \tag{5}$$

In medium -a < x < a (air gap), the solutions of Eq. (4) can for z and x components (using $\nabla.\vec{E}=0$, for x component of electric field) be written as

$$E_z = \left(A_{II}\exp(\alpha_{II}x) + A'_{II}exp(\alpha_{II}x)\right)exp\left[-i(\omega t - k_z z)\right],$$
$$E_x = -\frac{ik_z}{\alpha_{II}}\left[A_{II}\exp(\alpha_{II}x) + A'_{II}exp(-\alpha_{II}x)\right]exp\left[-i(\omega t - k_z z)\right]. \quad (6)$$

In Medium x > a, the solutions of Eq. (4) can for z and x components (using $\nabla.\vec{E}=0$, for x component of electric field) be written as

$$E_z = A_{III}exp(-\alpha_{III}x)exp\left[-i(\omega t - k_z z)\right],$$
$$E_x = A_{III}\frac{ik_z}{\alpha_I}exp(-\alpha_{III}x)exp\left[-i(\omega t - k_z z)\right]. \quad (7)$$

At boundaries x = -a and x = a, Eqs. (5)–(7) demand that

$$A_I exp(-\alpha_I a) = A_{II}exp(-\alpha_{II}a) + A'_{II}exp(\alpha_{II}a),$$
$$\epsilon_m\frac{\alpha_{II}}{\alpha_I}A_I = A_{II}exp(-\alpha_{II}a) + A'_{II}exp(\alpha_{II}a), \quad (8)$$

$$A_{II}exp(\alpha_{II}a) + exp(-\alpha_{II}a)A'_{II} = A_{III}exp(-\alpha_I a),$$
$$A_{II}exp(\alpha_{II}a) - A'_{II}exp(-\alpha_{II}a) = -\frac{\alpha_I\epsilon_m}{\alpha_I}A_{III}exp(-\alpha_I a). \quad (9)$$

For symmetrical mode (E_z is symmetric about x = 0), i.e., $A'_{II} = A_{II}$ and $A_{III} = A_I$, hence Eq. (9) gives the dispersion relation of SPs propagating in metal-air-metal symmetrical structure, i.e.,

$$\tanh(\alpha_{II}a) = -\frac{\alpha_{II}\epsilon_m}{\alpha_I}. \quad (10)$$

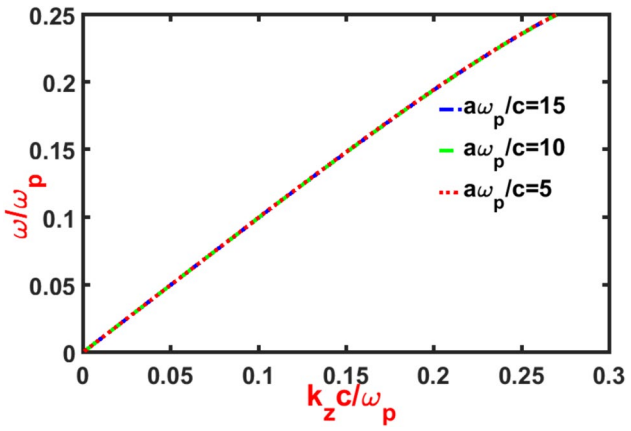

Fig. 2 Dispersion relation of surface plasmons in for metal-air-metal symmetrical structure for different values of air gap $a\omega_p/c = 5, 10, 15$ between metallic plates

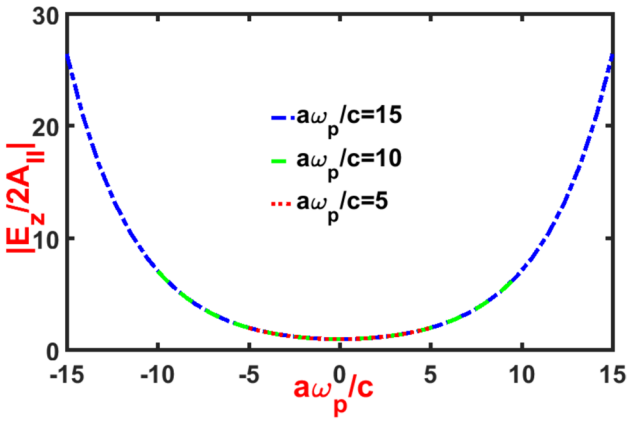

Fig. 3 Mode structure of SPs in metal-air-metal symmetrical structure for different values of air gap $a\omega_p/c = 5, 10, 15$ between metallic plates

The dispersion relation of Eq. (10) and mode structure of SPs Eqs. (5–7) are plotted in Figs. 2 and 3 for different normalized values of $a\omega_p/c = 5, 10, 15$ of the air gap between the metallic plates. Figure 2 shows that up to upper limit of SPs frequency, the frequency has linear behavior. For higher value of wavenumber, the curve has same behavior as that of single conductor surface. At the inter metallic surfaces of metal-air-metal structure, the SPs have maximum value and have zero inside the conductors (metallic plates) is shown in Fig. 3.

Terahertz Surface Plasmons Excitation by a Relativistic Electron Beam

Consider an electron beam of density n_{0b} and moving with relativistic velocity $v_{0b}\hat{z}$, through the air gap between two metallic plates (Fig. 4); the electron beam density is given by

$$n_{0b} = N_0 exp(-x^2/r_b^2), \quad (11)$$

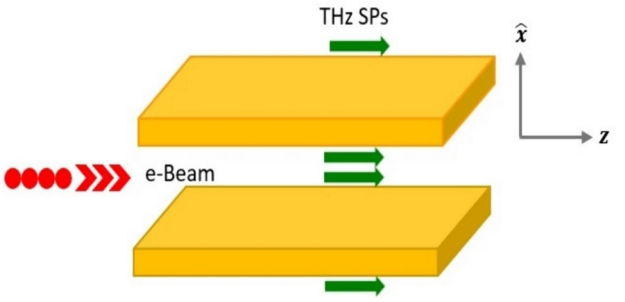

Fig. 4 THz surface plasmons excitation by a relativistic electron beam passing through the gap

where r_b is the radius of beam. The electron beam has a current is given by $I_b = \sqrt{\pi} N_0 abev_{0b}$, where b is the width of the electron beam. When this beam moves through the gap, it couples with the SPs. The response of electron beam in presence of SPs fields is given by the equation of motion

$$\left(\frac{\partial}{\partial t}\left(\gamma\vec{v}\right) + \vec{v}\cdot\nabla\left(\gamma\vec{v}\right)\right) = \frac{-e}{m}\left(\vec{E} + \frac{\vec{v}\times\vec{B}}{c}\right). \tag{12}$$

The electric and magnetic fields of SPs the air gap -a < x < a are given by

$$\begin{aligned}\vec{E} &= \left(A_{II}\left(\hat{z} - \frac{ik_z}{\alpha_{II}}\hat{x}\right)exp\left(\alpha_{II}x\right)\right.\\ &\quad\left. + A'_{II}\left(\hat{z} + \frac{ik_z}{\alpha_{II}}\hat{x}\right)exp\left(-\alpha_{II}x\right)\right)exp\left[-i\left(\omega t - k_z z\right)\right],\\ \vec{B} &= \hat{y}\frac{c}{i\omega}\frac{\omega^2}{c^2\alpha_{II}}(A_{II}\exp\left(\alpha_{II}x\right)\\ &\quad + A'_{II}exp\left(\alpha_{II}x\right))exp\left[-i\left(\omega t - k_z z\right)\right].\end{aligned} \tag{13}$$

The velocity of electron beam in the presence of SPs is given by $\vec{v} = v_{0b}\vec{z} + \vec{v}_1$ (beam velocity and perturbed velocity) and the Lorentz factor γ of the moving electron beam is given by $\gamma = \left(1 - \frac{v^2}{c^2}\right)^{-1/2}$ or $\gamma = \gamma_0 + \gamma_0^3\frac{v_{0b}\overrightarrow{v_{1z}}}{c^2}$. In terms of components and linearizing the Eq. (12), we have

$$\begin{aligned}&\frac{\partial}{\partial t}\left(\gamma_0 v_{1x}\hat{x} + \gamma_0^3 v_{1z}\hat{z}\right) + ik_z v_{0b}\left(\gamma_0 v_{1x}\hat{x} + \gamma_0^3 v_{1z}\hat{z}\right)\\ &= \frac{-e}{m}\left[\hat{x}\left(\left(1 - \frac{k_z v_{0b}}{\omega}\right)E_x + \frac{v_{0b}}{i\omega}\frac{\partial}{\partial x}E_z\right) + \hat{z}E_z\right].\end{aligned} \tag{14}$$

The x and z components of velocity of Eq. (14) can be written as $v_{1z} = \frac{eE_z}{im\gamma_0^3\left(\omega - k_z v_{0b}\right)}$,

$v_{1x} = \frac{eE_x}{mi\omega\gamma_0} - \frac{ev_{0b}}{m\omega\left(\omega - k_z v_{0b}\right)\gamma_0}\frac{\partial}{\partial x}E_z$. The equation of continuity is $\frac{\partial n}{\partial t} + \nabla\cdot\left(n\vec{v}\right) = 0$ where $n = n_{0b} + n_1$; this gives the perturbed density

$$n_{1=}\frac{\partial n_{0b}}{\partial x}\frac{v_{1x}}{i\left(\omega - k_z v_{0b}\right)}E_z + \frac{n_{0b}\nabla\cdot\overrightarrow{v_1}}{i\left(\omega - k_z v_{0b}\right)}. \tag{15}$$

The total perturbed current density is given by $\overrightarrow{J_1} = -n_{0b}e\overrightarrow{v_1} + n_1 ev_{0b}\hat{z}$. For purely growing instability, we look the terms that have $\left(\omega - k_z v_{0b}\right)^2$ in denominator and other terms may be discarded it. So, the total perturbed current density is given by

$$\begin{aligned}\overrightarrow{J_1} &= -\frac{\hat{z}ev_{0b}}{i\left(\omega - k_z v_{0b}\right)^2}\\ &\quad\left[-\frac{\partial n_{0b}}{\partial x}\frac{ev_{0b}}{m\omega\gamma_0}\frac{\partial}{\partial x}E_z - \frac{ev_{0b}n_{0b}}{m\omega\gamma_0}\frac{\partial^2}{\partial x^2}E_z + \frac{n_{0b}k_z eE_z}{m\gamma_0^3}\right],\end{aligned} \tag{16}$$

The Cherenkov condition demands that $k_z \approx \omega/v_{0b}$. In Eq. (16), the last two terms cancel out each other and one may get

$$\overrightarrow{J_1} = \frac{\hat{z}e^2 v_{0b}}{im\omega\gamma_0\left(\omega - k_z v_{0b}\right)^2}\frac{\partial n_{0b}}{\partial x}\frac{\partial E_z}{\partial x}. \tag{17}$$

At boundaries x = -a and x = a of interfaces in metal-air metal structure, the field of SPs satisfying the Maxwell's equations $\nabla\times\vec{E}_s = \frac{i\omega}{c}\vec{H}_s$, $\nabla\times\vec{H}_s = -\frac{i\omega}{c}\varepsilon'\vec{E}_s$, in the absence of electron beam. The permittivity has value $\varepsilon' = \varepsilon_m = \varepsilon_L - \omega_p^2/\omega^2$ in I (-a < x) and III (a > x). In the presence of moving electron beam, the new electric and magnetic fields of SPs are given by.

$$\vec{E} = A(t)\vec{E}_s,\ \vec{H} = B(t)\vec{H}_s. \tag{18}$$

The fields $\vec{E}$ and $\vec{H}$ of SPs both satisfy the Maxwell's equations inside the metals, which are given by $\nabla\times\vec{E} = -\frac{1}{c}\frac{\partial H}{\partial t}$, $\nabla\times\vec{H} = \frac{4\pi}{c}\left(\overrightarrow{J_{1b}} + \overrightarrow{J_{1p}}\right) = \frac{\varepsilon_L}{c}\frac{\partial\vec{E}}{\partial t}$, where $\overrightarrow{J_{ip}} = \sigma_m A\vec{E}_s + i\frac{\partial\sigma_m}{\partial\omega}\frac{\partial A}{\partial t}\vec{E}_s, \varepsilon_m = \varepsilon_L + i\frac{4\pi\sigma_m}{i\omega}$ and outside the metals $\varepsilon_L = 1, \sigma = 0$, using Eq. (18). We have

$$\frac{\partial B}{\partial t} = -i\omega(A - B), \tag{19}$$

$$\left[\frac{\partial A}{\partial t}\frac{\partial}{\partial\omega}\varepsilon'(\omega) - i\omega\varepsilon'(A - B)\right]\vec{E}_s = -4\pi\overrightarrow{J_{1b}}. \tag{20}$$

Putting Eq. (19) into Eq. (20) and assuming that $\partial B/\partial t \cong \partial A/\partial t$, the resulting equation is multiplying by E_s^* and integrating over the limit $-\infty to +\infty$, we have

$$\frac{\partial A}{\partial t} = \Gamma A = -2\pi\frac{\int_{-\infty}^{\infty} J_{1z}\cdot E_{sz}^* dz}{\int_{-\infty}^{\infty}\overrightarrow{E_s}\cdot\overrightarrow{E_s^*}dx} = R(A), \tag{21}$$

where $R(A) = -\frac{2\pi\int_{-a}^{a}\frac{\partial n_{0b}}{\partial x}\frac{\partial E_{sz}}{\partial x}E_{sz}^* dz\frac{e^2 v_{0b}^2}{im\omega\gamma_0\left(\omega - k_z v_{0b}\right)^2}}{\int_{-\infty}^{-a}\overrightarrow{E_s}\cdot\overrightarrow{E_s^*}dx + \int_{-a}^{a}\overrightarrow{E_s}\cdot\overrightarrow{E_s^*}dx + \int_{a}^{\infty}\overrightarrow{E_s}\cdot\overrightarrow{E_s^*}dx}$. In air gap -a < x < a, between metallic plates the electric field $\vec{E}_s$ of SPs is given by $\vec{E}_s = 2A_{II}\left(cosh\left(\alpha_{II}x\right)\hat{z} - \frac{ik_z}{\alpha_{II}}sinh\left(\alpha_{II}x\right)\hat{x}\right)exp\left[-i\left(\omega t - k_z z\right)\right]$ and using $\frac{\partial n_{0b}}{\partial x} = -\frac{2N_{0x}}{r_b^2}exp\left(-x^2/r_b^2\right)$, $\frac{\partial E_{sz}}{\partial x} = 2A_{II}\alpha_{II}sinh\left(\alpha_{II}x\right)exp[-i\left(\omega t - k_z z\right)]A$, the values of following terms are $\int_{-a}^{a}\frac{\partial n_{0b}}{\partial x}\frac{\partial E_{sz}}{\partial x}E_{sz}^* dz = -\frac{8N_0}{r_b^2}A_{II}^2\alpha_{II}^2 r_b^3\sqrt{\pi}/2$, $\int_{-a}^{a}\overrightarrow{E_s}\cdot\overrightarrow{E_s^*}dx == A_{II}^2\left(\frac{2}{\alpha_{II}}sinh\left(2\alpha_{II}a\right) + 4a\left(1 - \frac{k_z^2}{\alpha_{II}^2}\right)\right)$ and $\int_{a}^{\infty}\overrightarrow{E_s}\cdot\overrightarrow{E_s^*}dx = A_I^2\left(1 + \frac{k_z^2}{\alpha_I^2}\right)\int_{a}^{\infty}exp\left(-2\alpha_I x\right)dx = A_I^2\left(1 + \frac{k_z^2}{\alpha_I^2}\right)\frac{1}{2\alpha_I}exp\left(-2\alpha_I a\right)$, hence the RHS of Eq. (21) becomes $\frac{2\pi e^2 v_{0b}^2}{im\omega\gamma_0\left(\omega - k_z v_{0b}\right)^2}\frac{4N_0\alpha_{II}^2 r_{0b}\sqrt{\pi}}{\left(\frac{2}{\alpha_{II}}sinh\left(2\alpha_{II}a\right) + 4a\left(1 - \frac{k_z^2}{\alpha_{II}^2}\right) + \frac{A_I^2}{A_{II}^2}\left(1 + \frac{k_z^2}{\alpha_I^2}\right)\frac{1}{\alpha_I}exp\left(-2\alpha_I a\right)\right)}$. Using $\frac{A_I^2}{A_{II}^2} = 4exp\left(2\alpha_I a\right)cosh^2\left(\alpha_{II}a\right) = 2exp\left(2\alpha_I a\right)\left(1 + cosh\left(2\alpha_{II}a\right)\right)$, the RHS gives $\frac{2\pi e^2 v_{0b}^2 2N_0\alpha_{II}^2 r_{0b}\sqrt{\pi}}{im\omega\gamma_0\left(\omega - k_z v_{0b}\right)^2 D}$, where $D = sinh\left(2\alpha_{II}a\right) +$

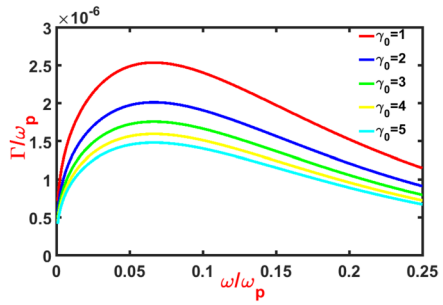

Fig. 5 Normalized growth rate Γ/ω_p as a function of normalized frequency ω/ω_p for the following parameters: $\omega_{pb}/\omega_p = 10^{-3}$; $v_{0b}/c = 10^{-2}$; $r_{0b}\omega_p/c = 10^{-5}$; $\varepsilon_L = 9$; for different relativistic energy $\gamma_0 = 1, 2, 3, 4, 5$ and normalized gap $a\omega_p/c = 5$

$\frac{\alpha_{II}}{\alpha_I}\left(1+\frac{k_z^2}{\alpha_I^2}\right)\left(1+cosh\left(2\alpha_{II}a\right)\right)+2\alpha_{II}a\left(1-\frac{k_z^2}{\alpha_{II}^2}\right)$, hence the Eq. (21) gives.

$$\frac{\partial A}{\partial t} = \frac{4\pi^{3/2}e^2v_{0b}^2N_0r_{0b}\alpha_{II}^3}{m\gamma_0\omega\left(\omega - k_zv_{0b}\right)D} \tag{22}$$

Taking $\partial A/\partial t = -i\delta, \omega = k_zv_{0b} + \delta$, one may obtain the $\delta^3 = R\,exp(2il\pi)$, where $R = \frac{4\pi^{3/2}e^2v_{0b}^2N_0r_{0b}\alpha_{II}^3}{m\gamma_0\omega D}$. Hence, the growth rate turns out to be, $\Gamma = im\delta = R^{1/3}\frac{\sqrt{3}}{2}$ and it gives

$$\Gamma = \frac{\sqrt{3}}{2}\left(\frac{\omega_{pb}^2v_{0b}^2r_{0b}\alpha_{II}^3}{\gamma_0\omega D}\right)^{1/3}. \tag{23}$$

The Eq. (23) gives the growth rate of THz SPs generation. The normalized growth rates versus normalized frequency of THz SPs for different energy values (γ_0) of an electron beam and different normalized

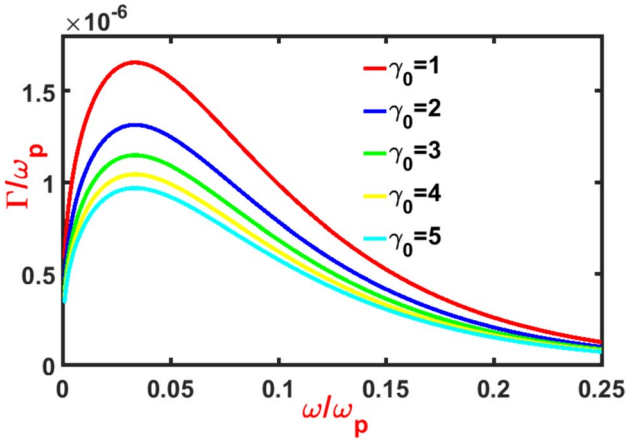

Fig. 6 Normalized growth rate Γ/ω_p as a function of normalized frequency ω/ω_p for the following parameters: $\omega_{pb}/\omega_p = 10^{-3}$; $v_{0b}/c = 10^{-2}$; $r_{0b}\omega_p/c = 10^{-5}$; $\varepsilon_L = 9$; for different relativistic energy $\gamma_0 = 1, 2, 3, 4, 5$ and normalized gap $a\omega_p/c = 10$

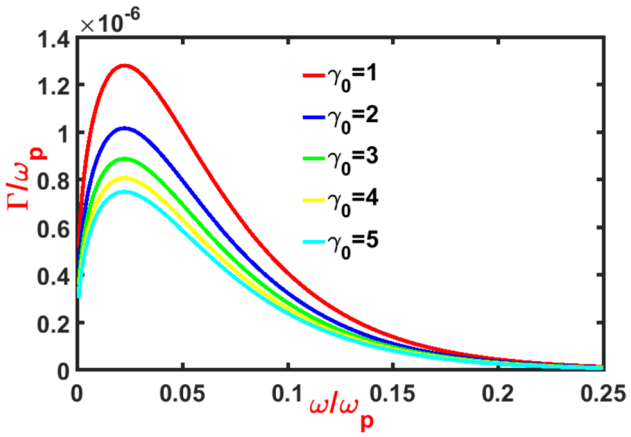

Fig. 7 Normalized growth rate Γ/ω_p as a function of normalized frequency ω/ω_p for the following parameters: $\omega_{pb}/\omega_p = 10^{-3}$; $v_{0b}/c = 10^{-2}$; $r_{0b}\omega_p/c = 10^{-5}$; $\varepsilon_L = 9$; for different relativistic energy $\gamma_0 = 1, 2, 3, 4, 5$ and normalized gap $a\omega_p/c = 15$

values of air gap ($a\omega_{p/c}$) between metallic plates is plotted in Figs. 5, 6, 7, and 8. We plotted the normalized growth rates for following parameters: $\omega_{pb}/\omega_p = 10^{-3}$; $v_{0b}/c = 10^{-2}$; $r_{0b}\omega_{p/c} = 10^{-5}$; $\varepsilon_L = 9$; for different energy values of electron beam $\gamma_0 = 1, 2, 3, 4, 5$ and air gap between metallic plates $a\omega_{p/c} = 5, 10, 15, 20$. Figures 5, 6, 7 and 8 show that there is board spectrum of THz radiation. The growth rate of THz radiation is lower for high energy electron beam as compared to low energy electron beam, because at low energy the electron beam has strong interaction with highly localized and propagating SPs. In Figs. 6, 7, and 8, it is shown that as

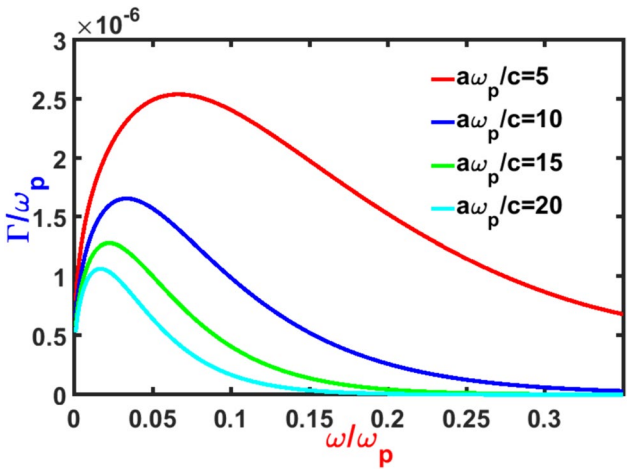

Fig. 8 Normalized growth rate Γ/ω_p as a function of normalized frequency ω/ω_p for the following parameters: $\omega_{pb}/\omega_p = 10^{-3}$; $v_{0b}/c = 10^{-2}$; $r_{0b}\omega_p/c = 10^{-5}$; $\varepsilon_L = 9$; for different values of normalized gap $a\omega_p/c = 5, 10, 15, 20$ and fixed energy of electron beam $\gamma_0 = 1$

increasing the air gap between the metallic plates, the growth rate is decreased. Figures 5, 6, 7 and 8 also show that the growth rate decreases with increases in the beam energy, frequency, and air gap between the plates.

Conclusion

In conclusion, the metal-air-metal symmetrical structure is a favorable structure for broadband THz radiation generation by relativistic electron beam (MeV). These beams are easily generated from plasma-based charged particle accelerators [39]. The growth rate and frequency have large value for low energy electron beam. The growth rate of generated THz radiation is varying with one third power of beam current density and peak of the growth rate at particular value of frequency is decided by the energy of electron beam and an air gap between the plates (few micron). The radiation frequency about 0.50 THz can be generated by an electron beam have current about 170 A and energy nearly about 3 MeV and has growth time is few ns. The highly confined and propagating THz SPs can be transformed into THz radiation by a suitable surface grating that are commonly used at present days. The beam current has value nearly about 170 A. Hence, the proposed structure will open the possibility to design a compact source for coherent and tuneable THz radiation generation in broad spectrum regime. When a background plasma is created by the beam, the mode structure is considerably modified, leading to a reduction in the growth rate, hence to the efficiency of the device. In addition, this proposed structure also provides a new way of controlling the propagation of THz-SPs, which are important for manipulation of optical waves. The feasible applications of this device will be useful for medical diagnostics and treatments with considerable advantages, etc.

Author Contribution All authors contributed equally to this work.

Funding There is no funding for this research work.

Data Availability No datasets were generated or analysed during the current study.

Declarations

Competing Interests The authors declare no competing interests.

References

1. Tonouchi M (2007) Cutting-edge terahertz technology. Nat Photonics 1:97
2. Mittleman D, Gupta M, Neelamani R, Baraniuk R, Rudd J, Koch M (1999) Recent advances in terahertz imaging. Appl Phys B 68(6):1085
3. Bergen MH, Lowry SN, Mitchell ME, Jenne MF, Collier CM, Holzman JF (2023) Terahertz wireless communication systems: challenges and solutions for realizations of effective bidirectional links. Opt Contin 2(10):2154–2177
4. Castro-Camus E, Koch M, Mittleman DM (2022) Recent advances in terahertz imaging: 1999 to 2021. Appl Phys B 128:12
5. Grischkowsky D, Keiding SR, Van Exter M, Fattinger Ch (1990) Far-infrared time-domain spectroscopy with terahertz beams of dielectrics and semiconductors. J Opt Soc Am B 7:2006
6. Nagel M, Haring Bolivar P, Brucherseifer M, Kurz H, Bosserhoff A, Büttner R (2002) Integrated THz technology for label-free genetic diagnostics. Appl Phys Lett 80:154
7. Huber R, Tauser F, Brodschelm A, Bichler M, Abstreiter G, Leitenstorfer A (2001) How many-particle interactions develop after ultrafast excitation of an electron-hole plasma. Nature 414:286
8. Ferguson B, Zhang X-C (2002) Materials for terahertz science and technology. Nat Mater 1:26
9. Siegel PH (2004) Terahertz technology in biology and medicine. IEEE Trans Microwave Theory Tech 52:2438
10. Mittleman DM, Hunsche S, Boivin L, Nuss MC (1997) T-ray tomography. Opt Lett 22:904
11. Son Joo-Hiuk, Seung Jae Oh, Cheon Hwayeong (2019) Potential clinical applications of terahertz radiation. J Appl Phys 125:190901
12. Zhang J, Li S, Le W (2021) Advances of terahertz technology in neuroscience. iScience 24(12):103548
13. Nanni EA, Huang WR, Hong KH, Ravi K, Fallahi A, Moriena G, Dwayne Miller RJ, Kärtner FX (2015) Terahertz-driven linear electron acceleration. Nat Commun 6:8486
14. Tang H, Zhao L, Zhu P, Zou X, Qi J, Ya Cheng, Qiu J, Xianggang Hu, Song W, Xiang D, Zhang J (2021) Stable and scalable multistage terahertz-driven particle accelerator. Phys Rev Lett 127:074801
15. Holzman JF, Elezzabi AY (2003) Two-photon photoconductive terahertz generation in ZnSe. Appl Phys Lett 83:2967
16. Ma GH, Tang SH, Kitaeva GKh, Naumova II (2006) Terahertz generation in Czochralski-grown periodically poled Mg:Y:$LiNbO_3$ by optical rectification. J Opt Soc Am B 23:81
17. Budiarto E, Margolies J, Jeong S, Son J, Bokor J (1996) High-intensity terahertz pulses at 1-kHz repetition rate. IEEE J Quantum Electron 32:1839
18. Happek U, Sievers AJ, Blum E (1991) Observation of coherent transition radiation. Phys Rev Lett 67:2962
19. Byrd JM, Hao Z, Mavtire MC, Robin DS, Sanmibale F, Schoenlein RW, Zholents AA, Zdotorev MS (2006) Laser seeding of the storage-ring microbunching instability for high-power coherent terahertz radiation. Phys Rev Lett 97:074802
20. Leemans WP, van Tilborg J, Faure J, Geddes CGR, Toth CS, Schroeder CB, Esarey E, Fubioni G, Dugan G (2004) Terahertz radiation from laser accelerated electron bunches. Phys Plasmas 11:2899
21. Ritchie RH (1957) Plasma losses by fast electrons in thin films. Phys Rev 106:874
22. Raether H (1988) Surface plasmons on smooth and rough surfaces and on gratings. Springer Tracts in Modern Physics. Springer-Verlag, New York
23. Maier SA (2007) Plasmonics: fundamentals and applications. Springer-Verlag, New York
24. Garcia-Vidal FJ, Martin-Moreno L, Pendry JB (2005) Surfaces with holes in them: New plasmonic metamaterials. J Opt A: Pure Appl Opt 7:S97
25. Berini P, De Leon I (2012) Surface plasmon–polariton amplifiers and lasers. Nat Photonics 6:16

26. Ebbesen TW, Lezec HJ, Ghaemi HF, Thio T, Wolff PA (1998) Extraordinary optical transmission through sub-wavelength hole arrays. Nature 391:667
27. Vampa G, Ghamsari BG, Siadat Mousavi S, Hammond TJ, Olivieri A, Lisicka-Skrek E, Yu Naumov A, Villeneuve DM, Staudte A, Berini P, Corkum PB (2017) Plasmon-enhanced high-harmonic generation from silicon. Nat Phys 13:659
28. Temnov VV (2012) Ultrafast acousto-magneto-plasmonics. Nat Photonics 6:728
29. Welsh GH, Hunt NT, Wynne K (2007) Terahertz-pulse emission through laser excitation of surface plasmons in a metal grating. Phys Rev Lett 98:026803
30. Maier SA, Andrews SR, Martın-Moreno L, Garcıa-Vidal FJ (2006) Terahertz surface plasmon-polariton propagation and focusing on periodically corrugated metal wires. Phys Rev Lett 97:176805
31. Liu S, Zhang C, Hu M, Chen X, Zhang P, Gong S, Zhao T, Zhong R (2014) Coherent and tunable terahertz radiation from graphene surface plasmon polaritons excited by an electron beam. Appl Phys Lett 104:201104
32. Liu S, Zhang P, Liu W, Gong S, Zhong R, Zhang Y, Hu M (2012) Surface polariton cherenkov light radiation source. Phys Rev Lett 109:153902
33. Shin H, Fan S (2006) All-angle negative refraction for surface plasmon waves using a metal-dielectric-metal structure. Phys Rev Lett 96:073907
34. Shin H, Yanik MF, Fan S, Zia R, Brongersma ML (2004) Omni-directional resonance in a metal–dielectric–metal geometry. Appl Phys Lett 84(22):4421
35. Andonian G, Stratakis D, Babzien M, Barber S, Fedurin M, Hemsing E, Kusche K, Muggli P, O'Shea B, Wei X, Williams O, Yakimenko V, Rosenzweig JB (2012) Dielectric wakefield acceleration of a relativistic electron beam in a slab-symmetric dielectric lined waveguide. Phys Rev Lett 108:244801
36. Kovalev NF, Nechaev VE, Petelin MI, Zaitsev NI (1998) Scenario for output pulse shortening in microwave generators driven by relativistic electron beams. IEEE Trans Plasma Sci 26(3):246
37. Pendry JJB, Holden AJ, Stewart WJ, Youngs I, Pendry B et al (1996) Extremely low frequency plasmons in metallic mesostructures. Phys Rev Lett 76:4773
38. Goebel DM, Butler JM, Schumacher RW, Santoru J, Eisenhart RL (1994) High-power microwave source based on an unmagnetized backward-wave oscillator. IEEE Trans Plasma Sci 22:547
39. Esarey E, Schroeder CB, Leemans WP (2009) Physics of laser-driven plasma-based electron accelerators. Rev Mod Phys 81:1229